ON EARTHQUAKE RESPONSE OF ELASTO-PLASTIC STRUCTURE CONSIDERING GROUND CHARACTERISTICS

by

T. Kobori(I), R. Minai(II) and Y. Inoue(III)

This paper is to discuss on the nonlinear response analysis of a coupled ground-structure system to earthquake type random excitations. The ground characteristics are represented by the approximate transfer function derived from the dynamical ground compliance and by the elasto-plastic boundary layer underneath the foundation mass as well. The results show that the nonstationary random response of the aboveground structure is inevitably influenced by energy dissipation in the boundary layer, energy radiation into the ground, and spectral characteristics of excitations.

1. Introduction

In the last several years there has been an increasing interest in the ground-structure interaction, that is one of the most important problems in earthquake engineering. In this paper, the nonlinear earthquake response analysis of the coupled ground-structure system subjected to earthquake type excitations is carried out by using an electronic analog computer in order to evaluate the interaction effect of the soil ground on the response of structure.

The earthquake type random excitations in this analysis, having a white spectrum and a finite duration-time are produced from the noise generator through a band-pass filter. And the coupled system consists of three models; an aboveground structure, an elasto-plastic boundary layer and a semi-infinite ground. In other words, the aboveground structure is idealized as a lumped mass-spring system with the bilinear hysteretic damping, the boundary layer near the periphery of the foundation mass is a very thin massless soil-layer where the plastic yielding occurs locally during strong earthquakes, and a semi-infinite ground is assumed to be a homogeneous, eleastic half-space having dynamical ground compliance approximated by the rational function type, linear transfer function. All the nonlinear earthquake responses are expressed in the nondimensional form defined as the ratio of the relative displacement of each part of this coupled system to the elastic limit deformation of the aboveground structure. And the average and standard deviation of the maximum responses for an ensemble of earthquake random excitations are evaluated. As an important result, it is found that the foundation with a boundary layer and a semi-infinite ground does accommodate the earthquake response of the aboveground structure to external energy arriving through the soil-ground.

(I) Prof. of Faculty of Eng., Kyoto Univ., Kyoto, JAPAN
(II) Prof. of Disaster Prevention Res. Inst., Kyoto Univ.
(III) Assist. Prof. of Disaster Prevention Res. Inst., Kyoto Univ.

2. Ground Compliance and Approximate Transfer Function

The dynamical ground compliance defined as the complex amplitude ratio of the displacement of a foundation to the harmonic exciting force has been studied under the various loading and ground conditions. In this section its compliance is approximately represented by the rational function type, linear transfer function, because it is necessary for the use of an analog computer in the nonstationary response analysis to transform the improper integral form or numerically plotted function of the dynamical ground compliance into a meromorphic function. For this purpose, let us consider the horizontal motion of a rectangular foundation on an elastic ground. The complex transfer function may be expressed as the ratio of the Fourier transform of the horizontal displacement of a foundation x_H to that of the applied horizontal force P_H as follows:

$$(1) \qquad \frac{\mathcal{F}[x_H]}{\mathcal{F}[P_H]} = \frac{1}{c\mu}\{f_{1H}(\omega') + j f_{2H}(\omega')\} = 1/b\mu K_H(j\omega') \quad , \omega' = b\Omega\sqrt{\frac{\rho}{\mu}} \quad , \quad j=\sqrt{-1}$$

in which b and c are half lengths of a rectangular foundation as in Fig. 1. ρ and μ denote the density and the shear modulus of the elastic ground, and Ω the angular frequency.

The complex-valued function, $f_{1H}(\omega') + j f_{2H}(\omega')$ or $K_H(j\omega')$, in Eq. (1) corresponds to the nondimensional dynamic ground compliance or stiffness, respectively. The ground compliance has been numerically evaluated as the function of the nondimensional frequency ω' , as defined by Eq. (1), the shape index of a rectangular foundation c/b , and Poisson's ratio of ground, under the assumption that the semi-infinite soil-ground is elastic and the shear stress distribution beneath the foundation mass is uniform because of the presence of the elasto-plastic boundary layer. Numerical values of the ground compliance calculated by a digital computer are shown as circle spots in Fig. 2 for the case where Poisson's ratio is $1/4$ and $c/b = 2$. For finding such an approximated transfer function yielding the minimum mean-squared error, we take the function $(b_1\omega'^2 + b_0)/(\omega'^4 + a_3\omega'^2 + a_0)$ to the real part and determine their coefficients. After considering the condition of physical realizability, we have the transfer function relevant to this coupled system in the form:

$$(2) \qquad \psi(s') = \frac{d_1 s' + d_0}{s'^2 + c_1 s' + c_0} \simeq \frac{c}{b}\,\frac{1}{K_H(s')}$$

in which $c_0 = 3.249$, $c_1 = 3.093$, $d_0 = 1.067$ and $d_1 = 0.157$. Using $s' = j\omega'$ in Eq. (2), we have the real and imaginary parts of the complex transfer function, which satisfy Hilbert transform pair, as shown by the two curves in Fig. 2.

The graphs in Fig. 3 indicate the amplitude characteristics of a rectangular foundation to ground motion when calculating through this transfer function, Eq. (2), for the nondimensional parameter $m_g = M_0/\rho b^3$ where M_0 is the foundation mass and ρ the density of elastic ground.

And the circle spots in Fig. 3 also represent the same amplitude characteristics produced from the numerical values of the circle spots in Fig. 2. According to these figures, it is evident that the approximated transfer function can be used henceforth with satisfactorily good accuracy.

3. Mathematical Model

There is a mathematical model which is essentially a ground-structure system coupled by the sub-system with energy consumption-radiation and dissipation. The sub-system consists of a rectangular foundation mass, a boundary layer and a semi-infinite ground. The above-ground structure system is, in common use at the present time, a shear type lumped system. The important point is obviously energy consumption in the sub-system, where the boundary layer underneath a foundation mass contributes to energy dissipation on account of the plastic yielding and the semi-infinite ground has radiation effect of seismic energy into the soil-ground. Thus a whole system is schematically shown as in Fig. 4. In this figure, M_i is the i th mass of the lumped system and M_0 the foundation mass. Φ_i and Φ_0 represent the bilinear restoring force characteristics, as shown in Fig. 5, of the i th story of the lumped system and those of the boundary layer, respectively. Φ_H is the dynamical ground stiffness corresponding to $K_H(j\omega)$ in Eq. (1). And Y_i, Y_0, Y_g and $\bar{Y}_H$ represent the absolute horizontal displacement of the i th mass, the foundation mass, boundary surface of elastic ground, and earthquake ground excitation, respectively.

Now the Laplace transforms of the equations of motion of the coupled ground-structure system are written in the nondimensional form

$$
\begin{aligned}
& m_i s^2 u_i + g_i(u_i - u_{i-1}) - g_{i+1}(u_{i+1} - u_i) = -m_i \hat{f} + \sigma_i \\
& u_{-1} = u_g \,, \quad u_n = u_{n+1} \,, \quad i = 0, 1, 2, \cdots n \\
& K_g K_H(qs) u_g - g_0(u_0 - u_g) = \sigma_g
\end{aligned}
\tag{3}
$$

where s is the complex parameter of the Laplace transformation associated with a nondimensional time variable τ, and σ_i, σ_0 and σ_g denote the inhomogeneous terms corresponding to the relevant initial conditions. The nondimensional variables τ and u_i and the inhomogeneous term $\hat{f}$ are defined as follows:

$$
\begin{aligned}
& \tau = \sqrt{\bar{K}/\bar{M}} \cdot T \,, \quad u_i = U_i - F_H \subset \eta_i = (Y_i - \bar{Y}_H)/\bar{\Delta} \\
& U_i \subset Y_i/\bar{\Delta} \,, \quad F_H \subset \bar{Y}_H/\bar{\Delta} \,, \quad \hat{f} = s^2 F_H \subset \alpha \cdot \hat{\alpha}(\tau) \\
& \alpha = A\bar{M}/\bar{K}\bar{\Delta} \,, \quad \hat{\alpha}(\tau) = \frac{d^2}{dT^2}(\bar{Y}_H/A)\Big|_{T=\tau\sqrt{\bar{M}/\bar{K}}} \,, \quad i = g, 0, 1, 2 \cdots n
\end{aligned}
\tag{4}
$$

where T is the time and A the maximum acceleration amplitude of ground. $\bar{M}$, $\bar{K}$, and $\bar{\Delta}$ denote the specific mass, stiffness and displacement respectively.

The functions g_i and g_0 in Eq. (3) are the Laplace transforms of nondimensional, bilinear restoring force characteristics of the lumped system and the boundary layer, respectively. Then we may write the following

relationship:

$$(5)\quad g_i \subset \kappa_i \varphi_i(\eta_i - \eta_{i-1};\ r_i,\ \delta_i) = \Phi_i(Y_i - Y_{i-1};\ K_{i1},\ K_{i2},\ \Delta_i)/\bar{B}$$
$$\eta_{-1} = \eta_g \quad , \quad Y_{-1} = Y_g$$

$$(6)\quad m_i = \frac{M_i}{\bar{M}} \quad , \quad \kappa_i = \frac{K_{i1}}{\bar{K}} \quad , \quad r_i = \frac{K_{i2}}{K_{i1}} \quad , \quad \delta_i = \frac{\Delta_i}{\bar{\Delta}} \quad , \quad i = 0, 1, 2 \cdots n$$

in which K_{i1}, K_{i2} and Δ_i as shown in Fig. 5 represent the first and second stiffness, and the elastic limit deformation, respectively. The specific value of strength $\bar{B}$ in Eq. (5) is equal to $\bar{K}\bar{\Delta}$. And a strength parameter β_i is defined by

$$(7)\quad \beta_i = \frac{B_i}{\bar{B}} = \frac{K_{i1}\Delta_i}{\bar{K}\bar{\Delta}} = \kappa_i \delta_i \quad , \quad i = 0, 1, 2, \cdots n$$

On the other hand, the linear transfer function, $K_H(qs)$ in Eq.(3) corresponds to the dynamic ground stiffness in Eq. (1), and by making use of the approximate transfer function of Eq. (2), we have

$$(8)\quad K_H(qs) = \frac{c}{b}\,\frac{(qs)^2 + c_1(qs) + c_0}{d_1(qs) + d_0} = K_H(s')$$

where q is the time parameter by which the nondimensional time τ' and the associated frequency parameter ω' defined by Eq. (1) are transformed into the nondimensional time τ and the corresponding frequency parameter ω Consequently $\tau = q\tau'$, $\omega = \omega'/q$, $\tau' = (1/b)\sqrt{\mu/\rho}\cdot T$ & $\omega = \Omega\sqrt{M/K}$.

Introducing the frequency ratio λ as the ratio of the fundamental natural frequency of the aboveground structure on the infinite rigid base, Ω_s to that of the ground-foundation system, Ω_g, then the parameter q is expressed by $q = \omega_s'/\omega_s = \lambda\omega_g'/\omega_g$ & $\lambda = \omega_s/\omega_g = \Omega_s/\Omega_g$, in which ω_g' is the function of Poisson's ratio of an elastic ground, the shape index of a rectangular foundation c/b and the mass ratio m_g defined as in the preceding section.

The specific nondimensional stiffness of the ground-foundation system κ_g appeared in Eq. (3) is expressed as $\kappa_g = b\mu/\bar{K} = m_0/m_g q^2$.

4. Nonstationary Earthquake Response Analysis

Without loss of generality, the aboveground structure may be simplified as a single-degree-of-freedom system having the pertinent ground characteristics, and the acceleration excitations of the earthquake type are represented by a set of sample functions of a band-limited white random process with a finite duration-time. Hence the nonstationary response analyses are to be carried out for the various sets of the system and excitation parameters. The key point in these analyses, of course, is evaluation of those parameters

of the actual system and excitations.

4.1 System Parameters: The mathematical model of the coupled ground-structure system is completely determined by specifying a set of nondimensional parameters defined by Eq. (3)~(8). In choosing the mass M_1, the first stiffness K_{11}, and the elastic limit deformation Δ_1, as the specific values of mass, stiffness and the deformation, respectively, and besides assuming the stiffness ratio r_1 defined by Eq. (6) to be o.1 appropriately, the nondimensional system parameters of the aboveground structure are $m_1 = 1$, $K_1 = 1$, $\delta_1 = 1$ & $r_1 = 0.1$. In addition, for the nondimensional foundation mass m_0 in Eq. (5) we choose $m_0 = 2$ & 0.8. Since it is somewhat difficult at the present time to presume the dynamic characteristics of a boundary layer, the gross values of the significant parameters K_0, β_0 and r_0 in Eqs. (6) and (7) are considered as $K_0 = 40, 20, 10, 4$, $\beta_0 = 1, 2$, $r_0 = 0.05$. Consequently the different values of the nondimensional elastic limit deformation in a boundary layer δ_0 for the various sets of K_0 and β_0 are introduced from Eq.(7). The mass ratio is assumed to be 1.6 and 32, so that the nondimensional fundamental natural frequency of ground-foundation system, ω_g for each value of m_g is calculated as 1.107 and 0.424, respectively. Let us suppose the values of the frequency ratio in the range of 0.2 to 1.6, then we have Table 1 for the numerical values of K_g.

According to those values of the system parameters, the amplitude characteristics of the elastic coupled system to the horizontal harmonic ground excitation, for instance, are calculated in the case where $\lambda = 0.6$ and $K_0 = 40$, for several sets of parameters m_0 and m_g in Figs. 6(a), (b) and (c). Considering the ground characteristics associated with the boundary layer and elastic ground, the natural periods of the coupled ground-structure system become undoubtedly longer than those of the aboveground structure on an infinitely rigid base, as shown in Fig. 7 for the fundamental natural period. Those periods can be calculated by the characteristic equation that is the sixth order algebraic equation derived from Eq. (3). A pair of conjugate complex eigen-values in each mode come from the roots of this characteristic equation, and the smallest absolute value of them gives a fundamental frequency. The equivalent critical damping ratio is given by the ratio of the positive value of the real part to the absolute value of the eigen-value (Fig. 8). The numerical values of the nondimensional fundamental natural frequency of the coupled system, in the case $\lambda = 0.2$, are given by Table 2 in which the values corresponding to the first stiffness of the bilinear hysteretic characteristics of a boundary layer are shown above in each box, and the values to the second stiffness below.

4.2 Generation of Excitations and Their Parameters: It is doubtlessly well-known among structural engineers that the nonstationary response of structures is to be extremely influenced with the spectral characteristics of earthquake excitations imposed at the ground. Therefore it is very important for this response analysis to select the pertinent ground accelerations or inputs expressed by a set of intensity and frequency parameters and even by a wave-shape function. We assume here as such inputs a a set of

sample functions of finite duration-time, Gaussian random process with a band-limited white spectrum, produced from the noise generator through a band-pass filter. The ratio of the upper limit frequency to the lower one in this filter is 50. And then the duration-time is chosen as 30 times as large as the shortest period corresponding to the upper limit frequency, or 0.6 times the longest period.

After generating thirteen wave-shape functions, each of them is digitized with sampling frequency about 68 times the upper limit frequency and the Fourier power spectrum defined as the time average of the squared absolute of the Fourier transform is calculated. Fig. 9 shows the average Fourier power spectra for two groups of thirteen and five wave-shape functions, weighted so that each time-function has the unit r.m.s. (i.e. root mean square). A set of nondimensional intensity and frequency parameters must be determined to perfectly describe an acceleration excitation in addition to the wave-shape function as given above. The intensity parameter defined in Eq. (4) is selected in the range of 0.4 to 2.0 so that the coupled system behaves in the elastic region up to the plastic region. In evaluating the average response spectra, the value of α associated with each random time-function is modified so that the r.m.s. of the time-function is equal to that of the standard time-function having the largest r.m.s. in the ensemble considered.

The frequency parameter ν is defined as the ratio of the upper limit frequency of excitations to the fundamental natural frequency of the above-ground structure on the rigid base; i.e. $\nu = \omega_u / \omega_s = \Omega_u / \Omega_s$ where Ω_u is the upper limit frequency of excitations. The value of ν is varied in the range of 2 to 20.

4.3 Definition of Responses: One of the key problems to approach anti-seismic design on a rational basis is the selection of a measure which guarantees the safey of structures against strong earthquakes. In this analysis the maximum nondimensional relative displacements of the above-ground structure, the boundary layer and the elastic ground, denoted by γ_{r1}, γ_{ro} and γ_{rg} are considered as follows:

$$(9) \qquad \gamma_{r1} = \frac{|Y_1 - Y_o|_{max}}{\bar{\Delta}} \quad , \quad \gamma_{ro} = \frac{|Y_o - Y_g|_{max}}{\bar{\Delta}} \quad , \quad \gamma_{rg} = \frac{|Y_g - \bar{Y}_H|_{max}}{\bar{\Delta}}$$

Since the elastic limit deformation of the aboveground structure is chosen as $\bar{\Delta}$ in Eq. (4), γ_{r1} means the maximum ductility ratio of the above-ground structure. On the other hand, the maximum ductility ratio of the boundary layer can be obtained dividing γ_{ro} by the nondimensional elastic limit deformation δ_o determined from Eq. (7).

In order to obtain the average and standard deviation of the maximum responses, the average maximum relative displacement of the aboveground structure, the boundary layer and the elastic ground denoted by $E\gamma_{r1}$, $E\gamma_{ro}$ and $E\gamma_{rg}$ are evaluated as the averages of γ_{r1}, γ_{ro} and γ_{rg} to thirteen and five different excitations, each having the same value of the intensity parameter α as described above. Similarly the standard deviations of the maximum responses are defined for these sets of excitations and they are

denoted by $\sqrt{V\gamma_{r1}}$, $\sqrt{V\gamma_{ro}}$ and $\sqrt{V\gamma_{rg}}$, respectively.

5. Discussion and Conclusion

The averages of the maximum nondimensional relative displacements of the ground-structure system subjected to thirteen different accelerations, each having the same r.m.s. and duration-time, are shown in Figs.10 and 11 for the intensity parameter α and the frequency parameter ν . For a small value of ν , the fundamental natural frequency of the coupled system lies in the center of the frequency band-width, so that the duration-time of excitations being relatively longer compared with the fundamental natural period. For a large ν , on the contrary, it lies close to the lower limit of the frequency band-width with the shorter duration-time. In these figures, the other variable system parameters except m_g are fixed as $\lambda = 0.2$, $m_o = 0.2$, $\kappa_o = 40$ & $\beta_o = 1$.

As shown in Figs. 10(a), (b) and (c), all the displacement responses increase as α increases, and the increasing rate of the response of each part of the coupled system is considerably influenced by the relevant ground characteristics as well as the excitation characteristics. In the case of relatively large ν , the average maximum relative displacement of the aboveground structure $E\gamma_{r1}$ increases gradually as α increases. In the case $\nu = 2$, however, the softening nonlinear characteristics and the resonant effect in a long duration-time make the response considerably large and unstable when α becomes large. As to the average response of the boundary layer $E\gamma_{ro}$, the elasto-plastic characteristics seem to have a little effect on the control of the response. The average response of the elastic ground $E\gamma_{rg}$ may be related to the restoring force characteristics of the boundary layer, because $E\gamma_{ro}$ could be regarded as an almost linear function of α .

In Figs. 11(a), (b) and (c) it is shown that each average displacement of the coupled system decreases monotonously as ν increases for each constant α . This tendency may be concerned with the fact that the maximum ductility ratio, defined as the ratio of the maximum relative displacement to the elastic limit deformation, of a single mass system subjected to random excitations is inversely proportional to the fundamental natural period in the elastic range for a constant α . The average responses, as a whole, seem to be smooth, monotonous functions of α and ν , although the response characteristics may be partially affected by the nonlinearity of the system and the nonstationary nature of the response as well as the spectral unevenness of excitations.

For two values of the mass ratio m_g , the responses $E\gamma_{r1}$ and $E\gamma_{ro}$ show no significant difference between the responses, while the response $E\gamma_{rg}$ depends remarkably on the parameter m_g . The value of $E\gamma_{rg}$ in the case where m_g =32.0 is about three times as large as that in the case where m_g = 1.6. In other words, the specific stiffness of elastic ground κ_g in the former case is about one third in the latter case.

The relation of the standard deviation to the average of thirteen responses is shown in Figs. 12(a), (b) and (c) for each displacement response of the coupled system. The dispersion in each ensemble of thirteen responses

may be quantitatively evaluated from the ratio of standard deviation to the average. It is found from Figs. 12(a), and (b) that the tendencies of the dispersion on the aboveground structure and boundary layer are similar to each other, and the standard deviation is nearly proportional to the average. And also, the ratio depending on the value of ν takes about 0.18 in the cases where $\nu = 2$ and 5, about 0.40 in the cases where $\nu = 10$, 15 and 20 for the aboveground structure, and about one and a half times these values for the boundary layer The reason why the ratio is larger in the low frequency range may arise from the facts that the response is greatly influenced by the local fluctuation of spectral characteristics in the individual excitation, and that the probability distribution of the responses spreads over large ν , for which the nonstationary nature is predominant because of the shorter duration-time of excitations as compared with the fundamental natural period.

As to the responses of an elastic ground, the results are somewhat complicated as shown in Fig. 12(c). These graphs may be explained by the facts that the standard deviation of those responses becomes so smaller as compared with the average, because the increments of the responses are obviously suppressed by the plastic yielding of the boundary layer, and that the standard deviation to the average increases again linearly when the responses at the second stiffness of the boundary layer are dominant.

In order to find the effect of the dynamic characteristics of the elastic ground on the response of the aboveground structure, the fundamental frequency ratio λ is varied in a wide range as shown in Figs. 13(a), (b) and (c) In these figures, the other variable parameters are taken as $m_o = 0.2$, $m_g = 32.0$, $\kappa_o = 40$, $\beta_o = 1$ and $\nu = 5$, and the average response is evaluated for five sample functions having the average Fourier power spectrum as shown by the dotted line in Fig. 9.

For the large value of λ , the coupled system has a long fundamental period relatively, otherwise the elastic ground is to be soft. Hence the duration-time of excitations is shorter as compared with the fundamental period, and also the equivalent critical damping ratio due to energy radiation is large as shown in Fig. 7. And the responses $E\gamma_{r1}$ and $E\gamma_{r0}$ have the tendency of decreasing with λ . Figs. 13(a) and (b) indicate that the linear or quasi-linear responses in the small range of α decrease smoothly, but they fluctuate with respect to λ for a large α since the nonlinear responses are apt to be influenced by the local fluctuation of the excitation spectrum. On the other hand, the response $E\gamma_{rg}$ increases with λ as shown in Fig. 13(c), since the stiffness of the ground-foundation system is inversely proportional to the square of λ . The effect of the stiffness seems to exceed that of the duration-time or energy radiation.

To clarify the influence of the dynamic properties of the subsystem on the response of the coupled system, the average responses of the system having several kinds of boundary layer are analyzed for five excitations. Supposing $\lambda = 0.2$, $m_g = 1.6$, $\nu = 5$ and $r_o = 0.05$, the stiffness parameter κ_o and the strength parameter β_o are varied. In addition, the mass ratio m_o is varied. Figs. 14 and 15 show the average responses of the coupled system in the cases where $m_o = 0.2$ and 0.8.

From Figs. 14(a) and 15(a) it is found that the response $E\gamma_{r1}$ is a little affected by the parameters κ_0 and m_0 as far as κ_0 is relatively large. And also the response $E\gamma_{r1}$ is considerably suppressed by the hysteretic energy dissipation at the boundary layer in the case where $\beta_0 = 1$. As shown in Figs. 14(b) and 15(b), the response $E\gamma_{r0}$ is remarkably influenced by the parameters describing the dynamic characteristics of the boundary layer. In these figures, when either κ_0 or β_0 becomes large and becomes small, the response $E\gamma_{r0}$ decreases and becomes stable. Furthermore, the increasing rate of the response $E\gamma_{r0}$ becomes large with α, dominated by m_0 rather than by β_0. It is notified that the maximum ductility ratio of the boundary layer seems to decrease as β_0 or $1/\kappa_0$ increases.

Figs. 14(c) and 15(c) indicate that the response $E\gamma_{rg}$ is remarkably suppressed by the plastic yielding of the boundary layer as α increases, and also it is much influenced by the parameter m_0 which is proportional to κ_g. From these figures it is found that the response $E\gamma_{rg}$ in the case where $m_0 = 0.2$ is about three times as large as that in the case where $m_0 = 0.8$, and for two values of m_0, the ratio of the response $E\gamma_{rg}$ differs considerably from the inverse ratio of κ_g. This may be interpreted by the effect of the inertia force acting on the subsystem and the damping effect due to the energy radiation into the ground. From these figures it is also found that the response $E\gamma_{rg}$ is not definitely influenced by the stiffness parameter κ_0 as compared with the distinct cut-off-effect caused by the decrease of the strength parameter β_0.

From the above discussions, the concluding remarks may be written as follows:

(1) In estimating the coupling effect of ground on the nonstationary nonlinear earthquake response of a ground-structure system, the approximate rational function type transfer function of the dynamical ground compliance of a foundation and the idealized boundary layer with nonlinear restoring force characteristics may be successfully applied to a reasonable mathematical model of the coupled system.

(2) The maximum relative displacement and the maximum ductility ratio of the structure are inevitably influenced by hysteretic energy dissipation of the boundary layer as well as energy radiation into the ground. This advantageous coupling effect of ground may be much more anticipated for the relatively rigid structures on the soft ground.

(3) In spite of the energy radiation into the soil-ground, the maximum relative displacement and ductility ratio of the boundary layer are apt to be large as the intensity of excitations increases, in the case where the strength of the bounday layer is smaller in comparison with that of the aboveground structure.

(4) It may be of great importance to evaluate reasonably the frequency and damping characteristics of the coupled system, particularly of a ground-structure system on the stratified ground, since the displacement response in the plastic range is sensitively influenced by the spectral characteristics of excitation.

(5) The maximum displacement of the elastic ground is closely related to the maximum shear force of the boundary layer and the increase of the displacement response is remarkably suppressed by the plastic yielding of the boundary layer. The hysteretic energy dissipation of the boundary layer seems to be profitable to the earthquake response of the structure, unless the large plastic behavior including the rotational or vertical deformation of the subsoil underneath the structure causes its unstability. It is, therefore, desirable to control the plastic deformation of the subsoil within a certain limit in an aseismic design of a ground-structure system.

Acknowledgement

We wish to thank Mr. T. Kamada, Research Assistant of Kyoto University, for his help in preparing this report.

REFERENCES

1. R. N. Arnold, G. N. Bycroft, and G. B. Warburton, Forced Vibrations on a Body of an Infinite Elastic Solid, Jour. of Applied Mech., Vol. 22, 1955, pp. 391-400.

2. I. Toriumi, Y. Sato and R. Yamaguchi, Vibrations in Foundation, Structure and its Vicinity on the Elastic Ground, Proc. of the Second World Conf. on Earthq. Eng., Japan, 1960, pp. 1413-1329.

3. W. T. Thomson and T. Kobori, Dynamical Compliance of Rectangular Foundation on an Elastic Half-Space, Jour. of Appl. Mech., Vol. 30, Series E, 1963, pp. 579-584.

4. T. Kobori, R. Minai, Y. Inoue and T. Kamada, Earthquake Response of the Structure Considering the Effect of Ground Compliance, Annuals, Disas. Prev. Res. Inst., Kyoto Univ., No. 10A, 1967, pp. 261-281.

5. W. T. Thomson, A. Survey of the Coupled Ground-Building Vibration, Proc. of the Second World Conf. on Earthq. Eng., Japan, 1960, pp. 833-847.

6. G. W. Housner and P. C. Jennings, Generation of Artificial Earthquake, Proc. of Am. Soc.of Civil Engs , Vol. 90 No. EM1, 1964, pp. 113-150.

7. T. Kobori, R. Minai and T. Suzuki, Dynamical Characteristics of Structures on an Elastic Ground, Annuals, Disas. Prev. Res. Inst., Kyoto Univ., No. 9, 1966, pp. 193-224.

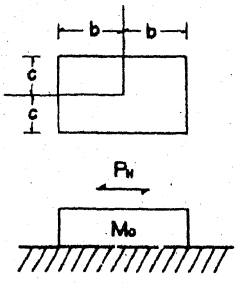

Fig.1 Ground-foundation system.

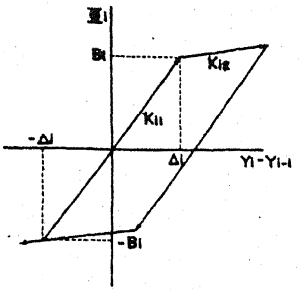

Fig.5 Bilinear restoring force characteristics.

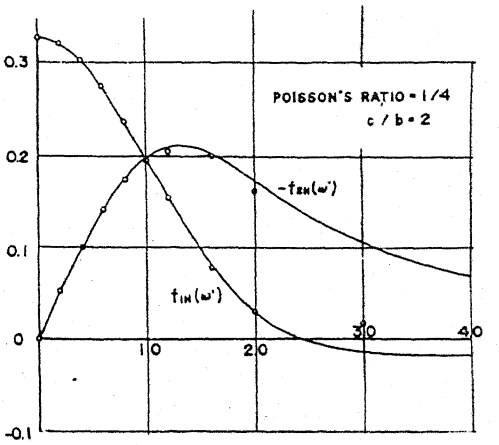

Fig.2 Nondimensional dynamic ground compliance, $f_{1H}(\omega') - j f_{2H}(\omega')$.

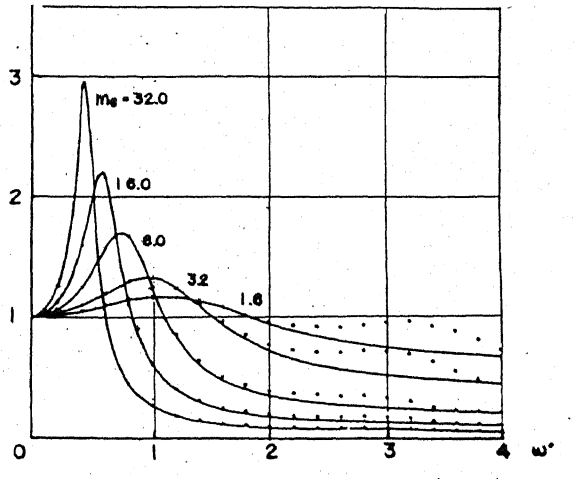

Fig.3 Amplitude characteristics of ground-foundation system.

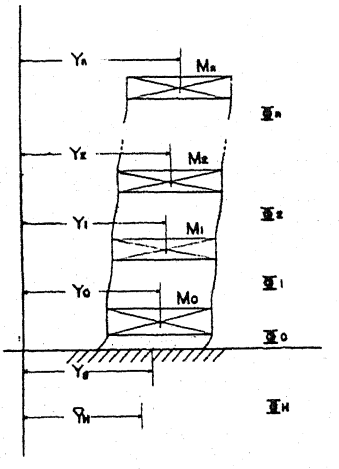

Fig.4 Model of ground-structure system.

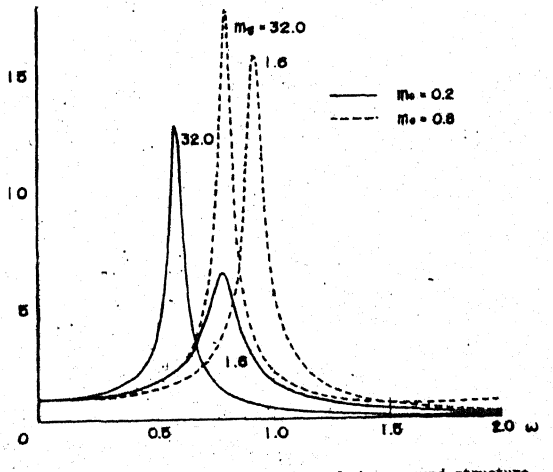

Fig.6 (a) Amplitude characteristics of aboveground structure.

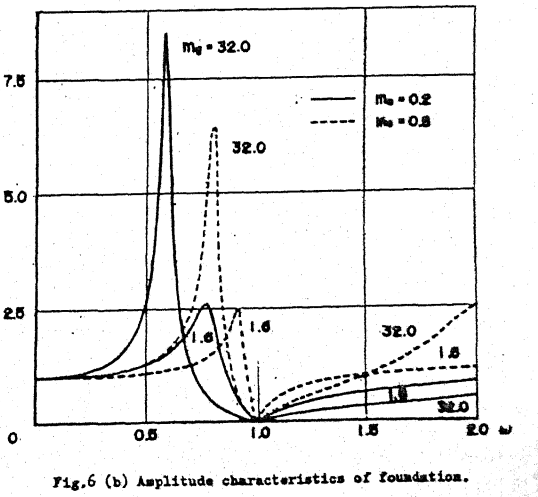

Fig.6 (b) Amplitude characteristics of foundation.

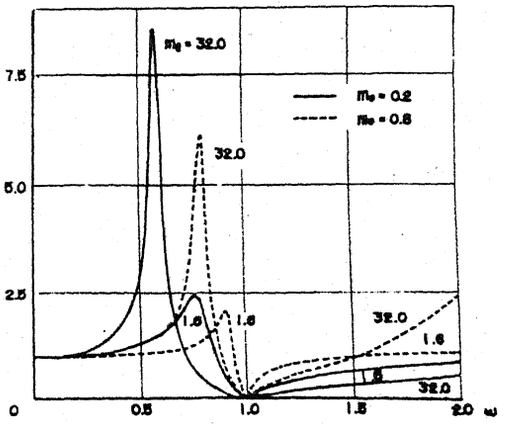

Fig.6 (c) Amplitude characteristics of elastic ground.

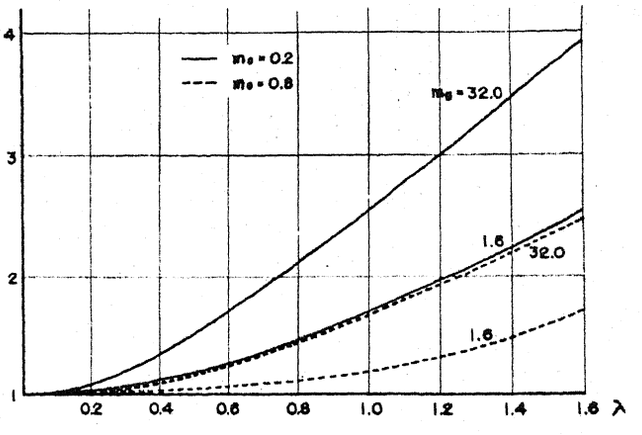

Fig.7 Fundamental natural period ratio.

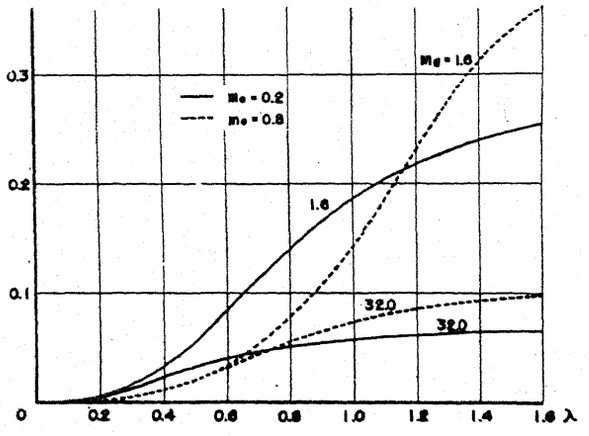

Fig.8 Equivalent critical damping ratio.

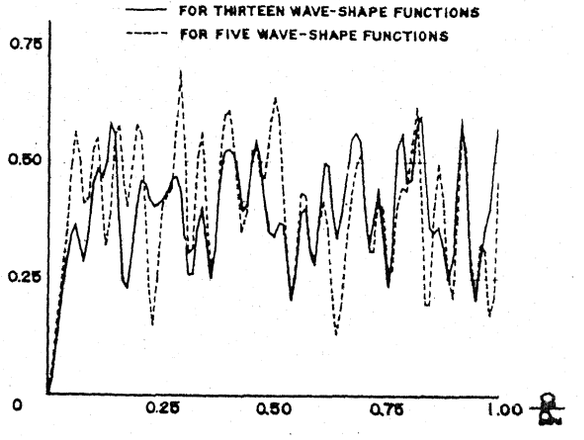

Fig.9 Average Fourier power spectra of acceleration excitations.

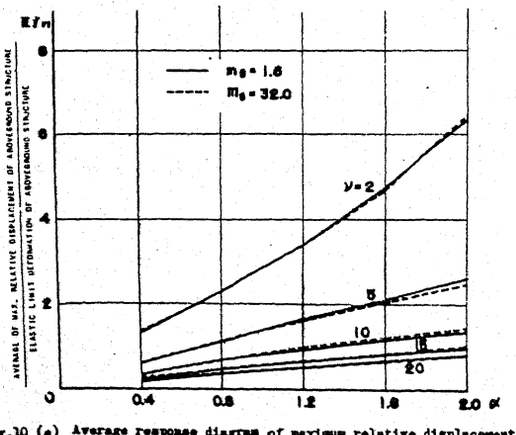

Fig.10 (a) Average response diagram of maximum relative displacement; $\lambda = 0.2$, $m_e = 0.2$, $K_e = 40$ and $A_e = 1$.

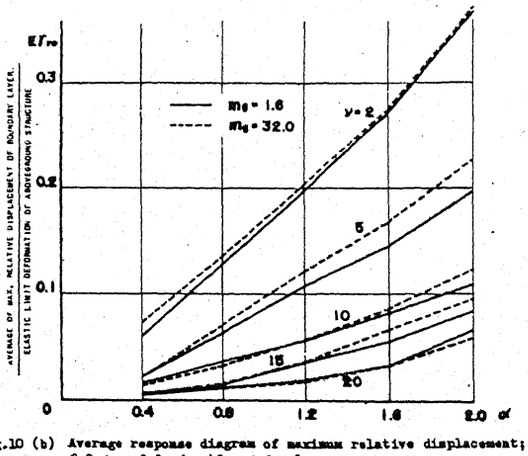

Fig.10 (b) Average response diagram of maximum relative displacement; $\lambda = 0.2$, $m_e = 0.2$, $K_e = 40$ and $A_e = 1$.

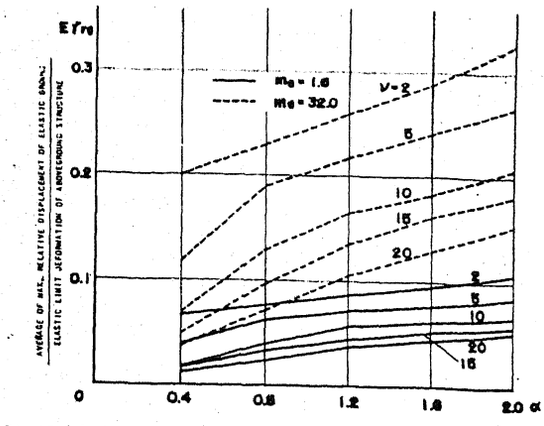

Fig.10 (c) Average response diagram of maximum relative displacement; $\lambda = 0.2$, $m_s = 0.2$, $K_s = 40$ and $\beta_s = 1$.

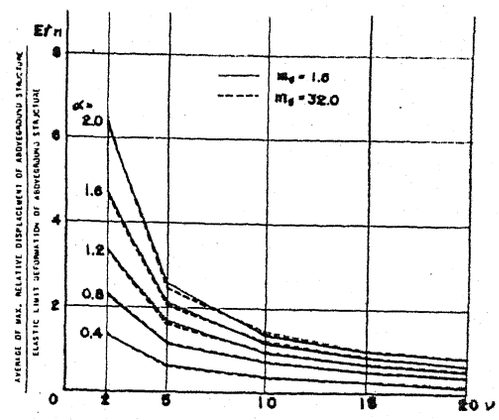

Fig.11 (a) Average response diagram of maximum relative displacement; $\lambda = 0.2$, $m_s = 0.2$, $K_s = 40$ and $\beta_s = 1$.

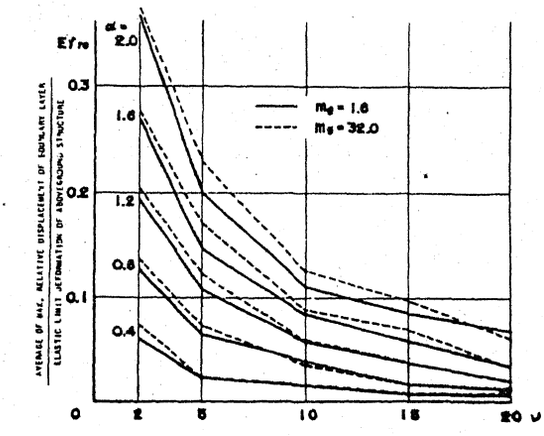

Fig.11 (b) Average response diagram of maximum relative displacement; $\lambda = 0.2$, $m_s = 0.2$, $K_s = 40$ and $\beta_s = 1$.

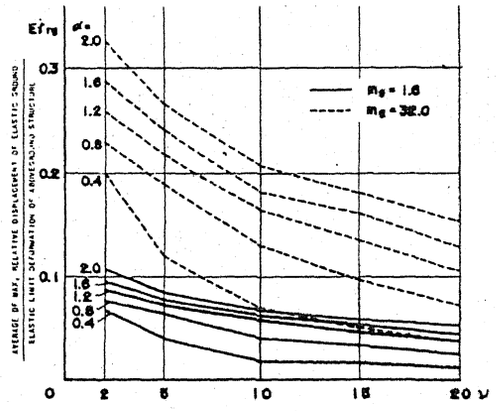

Fig.11 (c) Average response diagram of maximum relative displacement; $\lambda = 0.2$, $m_s = 0.2$, $K_s = 40$ and $\beta_s = 1$.

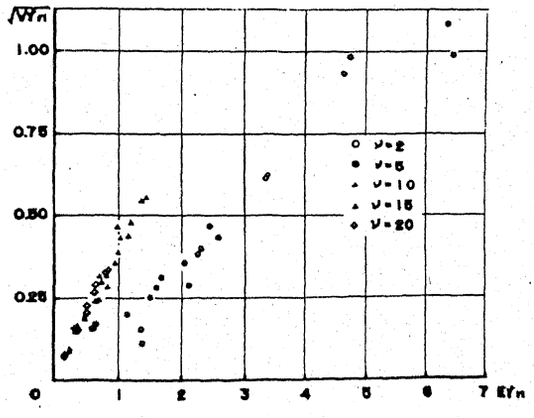

Fig.12 (a) Relation between standard deviation and average of maximum relative displacement; $\lambda = 0.2$, $m_s = 0.2$, $K_s = 40$ and $\beta_s = 1$.

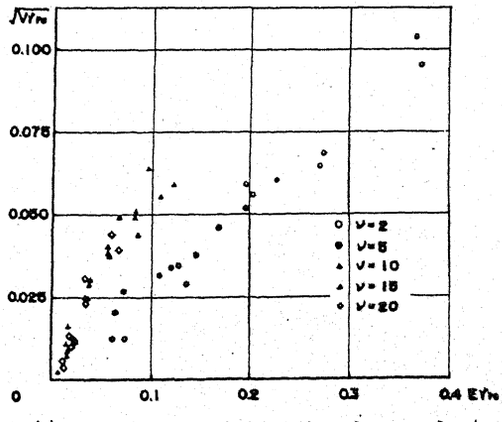

Fig.12 (b) Relation between standard deviation and average of maximum relative displacement; $\lambda = 0.2$, $m_s = 0.2$, $K_s = 40$ and $\beta_s = 1$.

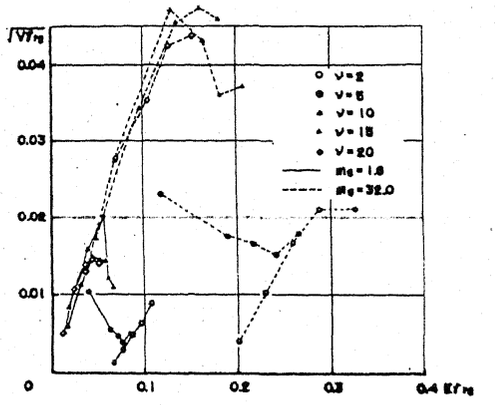

Fig.12 (c) Relation between standard deviation and average of maximum relative displacement; $\lambda = 0.2, m_0 = 0.2, K_0 = 40$ and $\beta_0 = 1$.

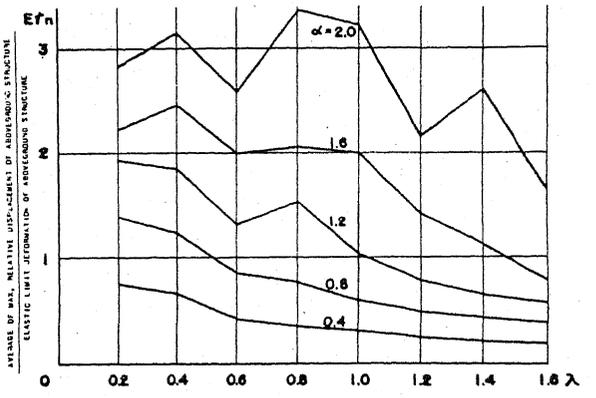

Fig.13 (a) Average response diagram of maximum relative displacement; $m_0 = 0.2, m_g = 32, K_0 = 40, \beta_0 = 1$ and $\nu = 5$.

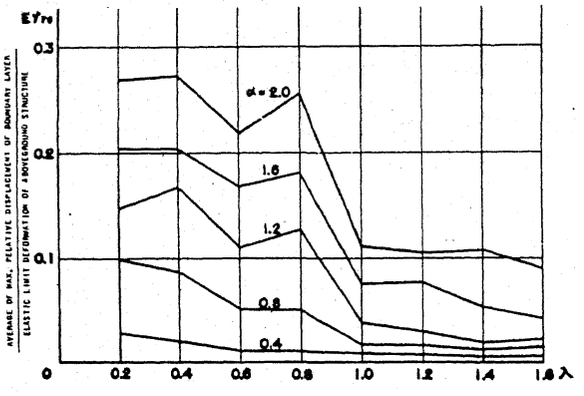

Fig.13 (b) Average response diagram of maximum relative displacement; $m_0 = 0.2, m_g = 32, K_0 = 40, \beta_0 = 1$ and $\nu = 5$.

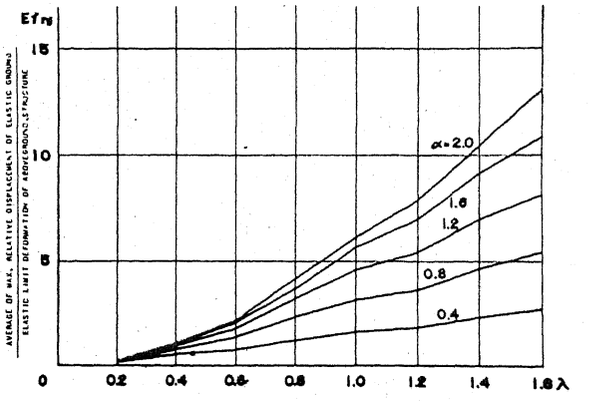

Fig.13 (c) Average response diagram of maximum relative displacement; $m_0 = 0.2, m_g = 32, K_0 = 40, \beta_0 = 1$ and $\nu = 5$.

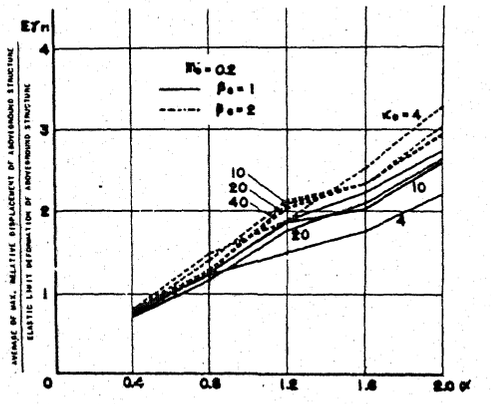

Fig.14 (a) Average response diagram of maximum relative displacement; $\lambda = 0.2, m_g = 1.6$ and $\nu = 5$.

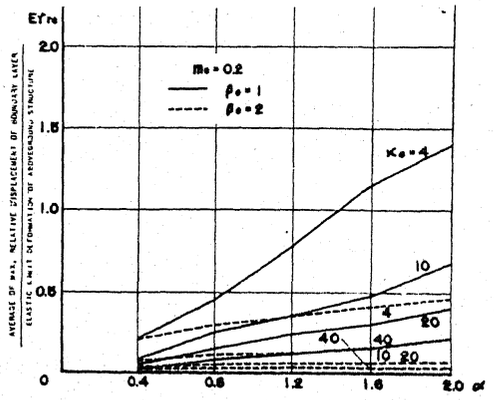

Fig.14 (b) Average response diagram of maximum relative displacement; $\lambda = 0.2, m_g = 1.6$ and $\nu = 5$.

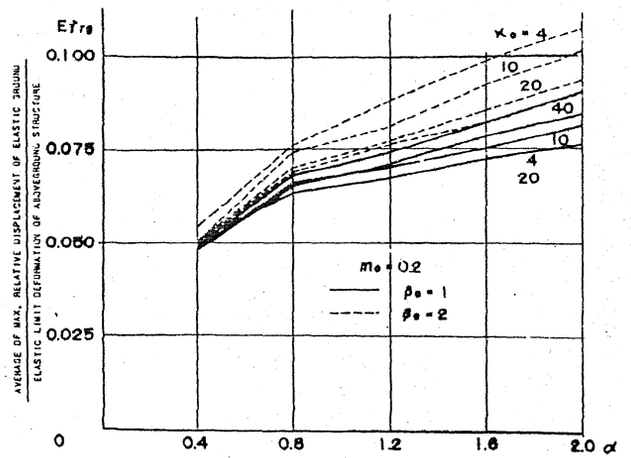

Fig.14 (c) Average response diagram of maximum relative displacement; $\lambda = 0.2$, $m_g = 1.6$ and $\nu = 5$.

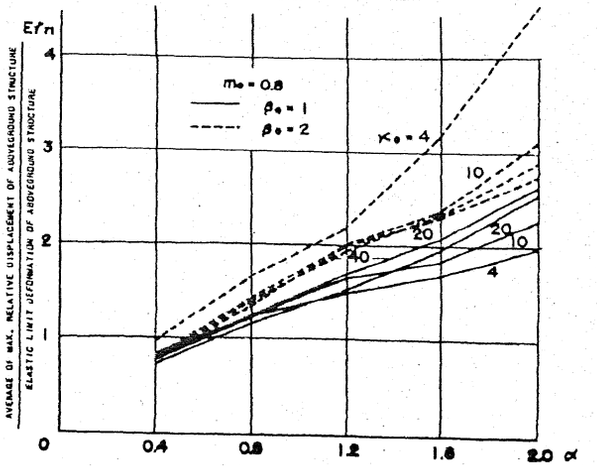

Fig.15.(a) Average response diagram of maximum relative displacement; $\lambda = 0.2$, $m_g = 1.6$ and $\nu = 5$.

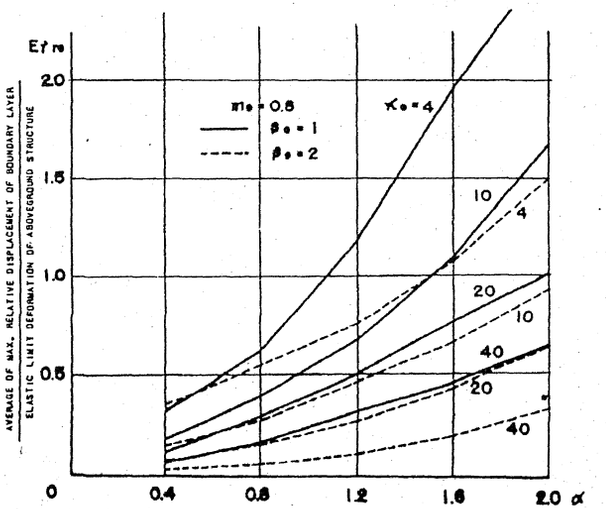

Fig.15 (b) Average response diagram of maximum relative displacement; $\lambda = 0.2$, $m_g = 1.6$ and $\nu = 5$.

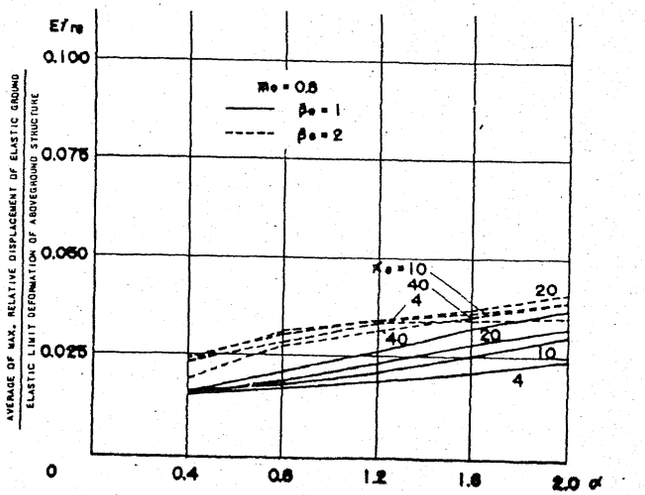

Fig.15 (c) Average response diagram of maximum relative displacement; $\lambda = 0.2$, $m_g = 1.6$ and $\nu = 5$.

Table 1 Nondimensional parameter K_g for $K_0 = 40$

m_0	0.2		0.8	
λ \ m_g	1.6	32.	1.6	32.
0.2	2.552	0.869	10.207	3.477
0.4	0.638	0.217	2.552	0.869
0.6	0.284	0.097	1.134	0.386
0.8	0.159	0.054	0.638	0.217
1.0	0.102	0.035	0.408	0.139
1.2	0.071	0.024	0.284	0.097
1.4	0.052	0.018	0.208	0.071
1.6	0.040	0.014	0.159	0.054

Table 2 Nondimensional fundamental natural frequency of the coupled system for $\lambda = 0.2$

	m_0	0.2		0.8	
K_0	$r_0 K_0$ \ m_g	1.6	32.	1.6	32.
40		0.958	0.906	0.980	0.964
	2.0	0.789	0.757	0.771	0.760
20		0.947	0.896	0.967	0.952
	1.0	0.678	0.656	0.632	0.625
10		0.926	0.877	0.942	0.927
	0.5	0.546	0.535	0.485	0.482
4		0.868	0.826	0.871	0.858
	0.2	0.380	0.376	0.326	0.322